Preprints.org

Article

Not peer-reviewed version

Antibacterial Activity of Biosynthesized Copper Oxide Nanoparticles (CuONPs) Using Ganoderma sessile

Karla M. Flores-Rábago , Daniel Rivera-Mendoza , Alfredo R. Vilchis-Nestor , Karla Juarez-Moreno , Ernestina Castro-Longoria *

Posted Date: 11 July 2023

doi: 10.20944/preprints202307.0734.v1

Keywords: green method; copper oxide nanoparticles; antibacterial; ultrastructure

Preprints.org is a free multidiscipline platform providing preprint service that is dedicated to making early versions of research outputs permanently available and citable. Preprints posted at Preprints.org appear in Web of Science, Crossref, Google Scholar, Scilit, Europe PMC.

Copyright: This is an open access article distributed under the Creative Commons Attribution License which permits unrestricted use, distribution, and reproduction in any medium, provided the original work is properly cited.

Preprints (www.preprints.org) | NOT PEER-REVIEWED | Posted: 11 July 2023 doi:10.20944/preprints202307.0734.v1

Disclaimer/Publisher's Note: The statements, opinions, and data contained in all publications are solely those of the individual author(s) and contributor(s) and not of MDPI and/or the editor(s). MDPI and/or the editor(s) disclaim responsibility for any injury to people or property resulting from any ideas, methods, instructions, or products referred to in the content.

Article

Not peer-reviewed version

Antibacterial activity of biosynthesized copper oxide nanoparticles (CuONPs) using Ganoderma sessile

Karla M. Flores-Rábago , Daniel Rivera-Mendoza , Alfredo R. Vilchis-Nestor , Karla Juarez-Moreno , Ernestina Castro-Longoria *

Posted Date: 11 July 2023

doi: 10.20944/preprints202307.0734.v1

Keywords: green method; copper oxide nanoparticles; antibacterial; ultrastructure

Preprints.org is a free multidiscipline platform providing preprint service that is dedicated to making early versions of research outputs permanently available and citable. Preprints posted at Preprints.org appear in Web of Science, Crossref, Google Scholar, Scilit, Europe PMC.

Copyright: This is an open access article distributed under the Creative Commons Attribution License which permits unrestricted use, distribution, and reproduction in any medium, provided the original work is properly cited.

© 2023 by the author(s). Distributed under a Creative Commons CC BY license.

Preprints (www.preprints.org) | NOT PEER-REVIEWED | Posted: 11 July 2023 doi:10.20944/preprints202307.0734.v1

Disclaimer/Publisher's Note: The statements, opinions, and data contained in all publications are solely those of the individual author(s) and contributor(s) and not of MDPI and/or the editor(s). MDPI and/or the editor(s) disclaim responsibility for any injury to people or property resulting from any ideas, methods, instructions, or products referred to in the content.

Article

Antibacterial Activity of Biosynthesized Copper Oxide Nanoparticles (CuONPs) Using *Ganoderma sessile*

Karla M. Flores-Rábago [1§], Daniel Rivera-Mendoza [1§], Alfredo R. Vilchis-Nestor [2], Karla Juarez-Moreno [3] and Ernestina Castro-Longoria [1,*]

[1] Department of Microbiology, Center for Scientific Research and Higher Education of Ensenada (CICESE), Carr. Tijuana-Ensenada 3918, Zona Playitas, 22860, Ensenada, Baja California, Mexico; riveramd@cicese.edu.mx (D.R.-M.).

[2] Sustainable Chemistry Research Joint Center UAEM—UNAM (CCIQS) Toluca-Atlacomulco Road Km 14.5, San Cayetano, Toluca 50200, Mexico.

[3] Center for Applied Physics and Advanced Technology, UNAM, Blvd. Juriquilla 3001, Juriquilla La Mesa, 76230, Juriquilla, Queretaro, Mexico; kjuarez@fata.unam.mx arvilchisn@uaemex.mx

* Correspondence: ecastro@cicese.mx

§ These authors contributed equally to this work.

Abstract: Copper oxide nanoparticles (CuONPs) were synthesized using an eco-friendly method and their antimicrobial and biocompatibility properties were determined. The supernatant and extract of the fungus *Ganoderma sessile* yielded small, quasi-spherical NPs with an average size of 4.5 ± 1.9 nm and 5.2 ± 2.1 nm, respectively. CuONPs showed antimicrobial activity against *Staphylococcus aureus, Escherichia coli* and *Pseudomonas aeruginosa*. Minimum inhibitory concentration (MIC) for *E. coli* and *S. aureus* was 15.9 µg/mL for nanoparticles (NPs) using the supernatant (CuONPs-S) and 16.5 µg/ml for NPs using the extract (CuONPs-E). Lower concentrations were required for *P. aeruginosa* inhibition. Ultrastructural analysis revealed the presence of the small CuONPs all through the bacterial cells. Finally, the toxicity of CuONPs was analyzed in three mammalian cell lines: hepatocytes (AML-12), macrophages (RAW 264.7) and kidney (MDCK). Low concentrations (<15 µg/ml) of CuONPs-E were non-toxic to kidney cells and macrophages, and the hepatocytes were the most susceptible to CuONPs-S. The results obtained suggest that the CuONPs synthesized using the extract of the fungus *G. sessile*, could be further evaluated for the treatment of superficial infectious diseases.

Keywords: green method; copper oxide nanoparticles; antibacterial; ultrastructure

1. Introduction

Bacterial resistance and multi-resistance to antibiotics is a global public health problem that is continuously growing. In the last decades, nanotechnology has contributed to possible solutions for the management of bacterial resistance to antibiotics, and with new methods for diagnosis and handling of diseases [1–5]. The antimicrobial and antioxidant properties of metal and metal oxide nanoparticles (NPs) are promising for multiple applications in different areas of medicine [6–9]. It has been documented that their antibacterial effect to combat bacterial resistance to antibiotics is promising [10,11]. However, the cytotoxic effect on animal cells has limited the applications to combat resistant bacteria [12,13]. For this reason, in recent decades, alternative nanocomposites with outstanding biocompatibility, lower cytotoxicity, and immunogenicity have been sought [14,15].

The implementation of the biological methods, also called "green methods", for the biosynthesis of metal and metal oxide NPs, have been extensively explored since they cause less damage to the environment, compared to chemical and physical methods, and could improve the effectivity and biocompatibility of nanomaterials [16–21].

The use of fungi to synthesize NPs holds particular interest, since fungi secrete large amounts of enzymes and metabolites and are easier to manipulate in the laboratory [22]. For instance, the synthesis of metal and metal oxide NPs using fungi has been studied and reported for over two

© 2023 by the author(s). Distributed under a Creative Commons CC BY license.

Preprints (www.preprints.org) | NOT PEER-REVIEWED | Posted: 11 July 2023 doi:10.20944/preprints202307.0734.v1

decades [22–24]. The intracellular compounds of the fungus as well as the compounds excreted into the medium (extracellular compounds) can be successfully used to produce NPs [25,26]. One of the benefits of using fungi for synthesizing metal-based NPs is that they do not require reducing chemical agents, protective agents, and/or stabilizing agents, which can be toxic [22].

For biomedical applications, silver and gold NPs have been the most studied, however NPs such as copper oxide, iron oxide and zinc oxide are currently being considered [27–30]. Recently, the production of copper and copper oxide NPs has gained interest, since in recent studies they have been shown to be useful for biomedical applications because of their anticancer, antioxidant, antimicrobial, and antidiabetic properties [9,18,31–33].

In this work, copper oxide nanoparticles (CuONPs) were produced using the extract and supernatant of *Ganoderma sessile*; this fungus is considered non-pathogenic to plants, animals or humans, is easy to handle and has a low production cost. Furthermore, mushrooms of the *Ganoderma* genus are considered medicinal, with antioxidant, anti-inflammatory and antitumor properties [34,35]. In addition, it has been shown that the extract and the supernatant of liquid cultures of *G. sessile* are not toxic to mammalian cell lines [26]. Therefore, the objective of the present study was to synthesize copper oxide NPs (CuONPs) using an eco-friendly method and to determine their antibacterial properties, seeking alternative methods to combat human pathogens.

2. Materials and Methods

2.1. Strain, media and growth conditions

Ganoderma sessile was obtained from the fungal stock of the Microbiology Department (CICESE). The strain was inoculated in Petri plates with potato dextrose agar medium (PDA) and incubated at 30 °C for 96 h. Once the mycelium filled ¾ of the culture dish, 10 plugs of the mycelium were taken with a standard size of 10 mm in diameter using a sterile borosilicate tube. The plugs were transferred to 250 mL Erlenmeyer flask with 100 mL of potato dextrose broth medium (PDB), and placed in an incubator with shaking at 120 rpm for 7 days at 30 °C.

2.2. Obtention of fungal supernatant and extract

To obtain fungal supernatant, the biomass obtained from liquid cultures was washed with sterile distilled water and placed in Erlenmeyer flasks with sterile deionized water in a 1:2 proportion (w/v) and incubated at 120 rpm for 24 h at 30 °C. After 24 hours, the supernatant was obtained by filtration through a nitrocellulose membrane with a pore size of 0.45 µm (MF-Millipore) and subsequently through a nitrocellulose membrane with a pore size of 0.22 µm (MF-Millipore), to eliminate all biomass.

Fungal extract was obtained using biomass from liquid cultures in a 1:1 proportion (w/v); biomass was washed with sterile distilled water and macerated with sterile deionized water using an agate mortar. Once macerated, it was centrifuged for 15 min at 10,000 rpm at 22 °C, and finally the aqueous extract was decanted. The extract obtained was filtered as described above.

2.3 Biosynthesis of copper oxide nanoparticles (CuONPs)

CuONPs were synthesized using fungal extract and/or supernatant mixed with pentahydrated copper sulfate ($CuSO_4.5H_2O$) 5 mM (Sigma-Aldrich, St. Louis, MI, USA) as follows: Copper sulfate : fungal supernatant (S) or extract (E) were mixed in a 3:1 proportion, pH was adjusted to 10 with NaOH (10 mM), then the resulting suspension was incubated for 24 h at 60 °C.

2.4 Characterization of CuONPs

CuONPs were analyzed by UV-Vis spectroscopy at 200 to 800 nm [32] in a Perkin Elmer precisely UV-Vis lambda/25 spectrophotometer (PerkinElmer Inc.,Waltham, MA, USA). Further characterization was carried out to determine the hydrodynamic diameter (HD), the zeta potential (ZP) and the polydispersity index (PDI) using a Zetasizer Nano ZS instrument (Malvern Panalytical

Preprints (www.preprints.org) | NOT PEER-REVIEWED | Posted: 11 July 2023 doi:10.20944/preprints202307.0734.v1

Inc., Westborough, MA, USA). Nanoparticles were analyzed under transmission electron microscopy (TEM) (Hitachi H7500, Hitachi Ltd., Tokyo, Japan) at 100 kV for size and shape determination. Also, CuONPs were examined using a high-resolution transmission electron microscope (HRTEM) (JEM-2100 from JEOL, JEOL Ltd., Tokyo, Japan) operated at 200 kV. To assess mean size of NPs, the ImageJ program (free version forWindows 1.8.0_172) was used.

2.5. X-ray diffraction (XRD) Analysis of Synthesized CuONPs

The structural analysis was performed by X-ray diffraction using a Bruker D8 Advanced diffractometer equipped with Linxeye Detector. The XRD pattern were collected with Cu Kα radiation and 2θ scanning angle variation between 10° and 80°. The phase analysis was supported with PDF-2 software.

2.6. Fourier Transform Infrared Spectroscopic (FTIR) Analysis of Synthesized CuONPs

To identify the functional groups that could be participating in the formation and stabilization of copper oxide nanoparticles, the samples were centrifuged, then the precipitates were collected and subsequently lyophilized. The FTIR spectra were acquired using a Bruker Tensor 27 spectrometer with Total Attenuated Reflectance (FTIR-ATR) in a range of 4000 cm^{-1} to 400 cm^{-1} in transmittance mode.

2.7. Evaluation of Antibacterial Activity

Antibacterial activity of the synthesized CuONPs was evaluated against *Escherichia coli* (ATCC 25922), *Staphylococcus aureus* (ATCC 25923) and *Pseudomonas aeruginosa* (ATCC 27853) as the minimum inhibitory concentration (MIC). For this, the plate microdilution assay was used, following the protocol of the Clinical and Laboratory Standards Institute [36]. For the microdilution assay, each bacterial strain was inoculated in Petri dishes with LB agar medium at 37 °C for 24 h. Subsequently, four colonies were inoculated in Mueller Hinton broth (MHB) and incubated at 37 °C under agitation, until reaching an approximate concentration of $5x10^5$ CFU / mL [36]. Then, the MIC determination was carried out in Polystyrene 96-Well microplates (Costar 3595). In each well, 50 µL of MHB was placed, and the different concentrations of CuONPs-S and CuONPs-E used, then 5 µL of the bacterial inoculum were added. MHB without inoculation and MHB with bacterial inoculum without CuONPs, were used as controls. The plates were incubated at 37 °C for 24 h. For the analysis, the Multiskan Sky version 1.00.55 plate reader (Thermo Scientific™) was used, with the Skanlt 6.0.1 software. After the incubation time, 10 µL of each well were inoculated in Petri dishes with LB agar and incubated for 24 to 48 h at 37 °C to determine bacterial growth (% CFU), the assays were done in triplicate.

2.8. ROS production in bacteria

To evaluate the production of reactive oxygen species (ROS) in bacteria, the following protocol was carried out: in a 96-well plate cells were seeded at $1×10^5$ cells per well, and exposed to different CuONPs concentrations (19.9, 9.95, 4.97, 2.48, 1.24, 0.62 µg/mL), followed by incubation at 37 °C for 24 h. Bacteria incubated with 1 mM of H_2O_2 were considered as a positive control, and as negative control cells without CuONPs were used.

After the treatment with CuONPs, cells were washed thrice with 200 µL of PBS 1× and incubated at 37°C in darkness with 100 µl of DCFDA (20,70-dichlorofluorescein diacetate, 45 µM) (D6883 Sigma-Aldrich) for 60 min. Fluorescence (λex = 485 nm and λem = 520 nm) was measured using a Cary Eclipse fluorescence spectrophotometer (Agilent Technologies CA, USA).

2.9. Ultrastructural analysis of bacteria

The interaction of CuONPs with bacteria was analyzed for Gram-negative *E. coli* and Gram-positive *S. aureus*. Strains were grown in MHB with CuONPs at the MIC obtained for each strain, also control cultures were prepared using the following protocol: After incubation for 24 h, cells were

Preprints (www.preprints.org) | NOT PEER-REVIEWED | Posted: 11 July 2023 doi:10.20944/preprints202307.0734.v1

fixed with 2.5% glutaraldehyde in 0.05 M sodium phosphate for 30 min. at ambient temperature. Then, cells were post-fixed with 2% OsO_4 at 4 °C for 2 h. Subsequently, samples were dehydrated in ethanol series and then infiltrated in Spurr resin/ethanol according to [38]. Samples were then polymerized at 60°C for 24 h, afterwards sections of 70 nm thick were obtained in a Leica Ultracut-R ultramicrotome (Leica Microsystems Inc., Buffalo Grove, IL, USA). Samples were mounted in formvar/carbon 75 mesh copper grids and analyzed under TEM (Hitachi H7500), operated at 100 keV. For better CuONPs detection, sections were not post-stained.

2.10. Effect of CuONPs in mammalian cell lines

The effect of CuONPs in cell lines was evaluated in the Madin-Darby canine kidney cell line (MDCK), a macrophage cell line (RAW 264.7) and a hepatocyte cell line (AML-12). To determine the susceptibility of the different cell lines to CuONPs, a 96-well microplate was used, each well containing 10,000 cells in a final volume of 100 µL. Cells were incubated at 37 °C with 5% CO_2 for 24 h. After incubation, the culture medium was discarded and the cells were exposed to different volumes of CuONPs (22.2, 11.1, 5.55, 2.775, 1.385 and 0.687 µL), obtained with the aqueous extract and supernatant of *G. sessile*. DMEM culture medium without CuONPs was the positive control, and 1% Triton X-100 in PBS was the negative control. The final volume of the wells was adjusted to 100 µL with supplemented DMEM medium, and the plate was incubated at 37 °C with 5% CO_2. After 24 h of incubation with CuONPs, the culture medium was discarded, and the cultures were washed three times with 200 µL of PBS. To determine cell viability, the colorimetric method of the reduction of (3-[4,5-dimethylthiazol-2-yl]-2,5 diphenyl tetrazolium bromide) (MTT) was used (Sigma Aldrich M-8910). The absorbance was read with a UV-vis spectrophotometer (Thermo Scientific Multiskan GO) at 570 nm and 690 nm. All MTT reduction assays were performed independently in triplicate.

2.11. Statistical analysis

Statistical analysis was performed using the GraphPad Prism 9.3.0 software. The average size of NPs was calculated measuring 1000 NPs of each sample. Plotted data were reported as mean ± standard deviation. Two-way ANOVA followed by a Tukey test was used to detect significant differences in the mammalian cell viability assays.

3. Results

3.1. Nanoparticle characterization

After incubation, CuONPs were firstly evaluated by UV-Vis spectroscopy. Synthesized NPs using the supernatant (CuONPs-S) displayed a dark blue color, maximum absorbance peak was observed at 290.73 nm (Figure 1A). Nanoparticles were polydisperse (PDI = 0.619), quasi-spherical in shape (Figure 1B) and had a mean size of 4.5 ± 1.9 nm with a size range of 1-15 nm (Figure 1C) and zeta potential of –28.7 mV (Figure 1D). The negative value of the Z-potential can be attributable to the nature of the biomolecules involved in the stabilization of the nanoparticles, a larger negative value of Z-potential in nanoparticles usually indicates good stability of the suspension due to electrostatic repulsion between nanoparticles.

Preprints (www.preprints.org) | NOT PEER-REVIEWED | Posted: 11 July 2023 doi:10.20944/preprints202307.0734.v1

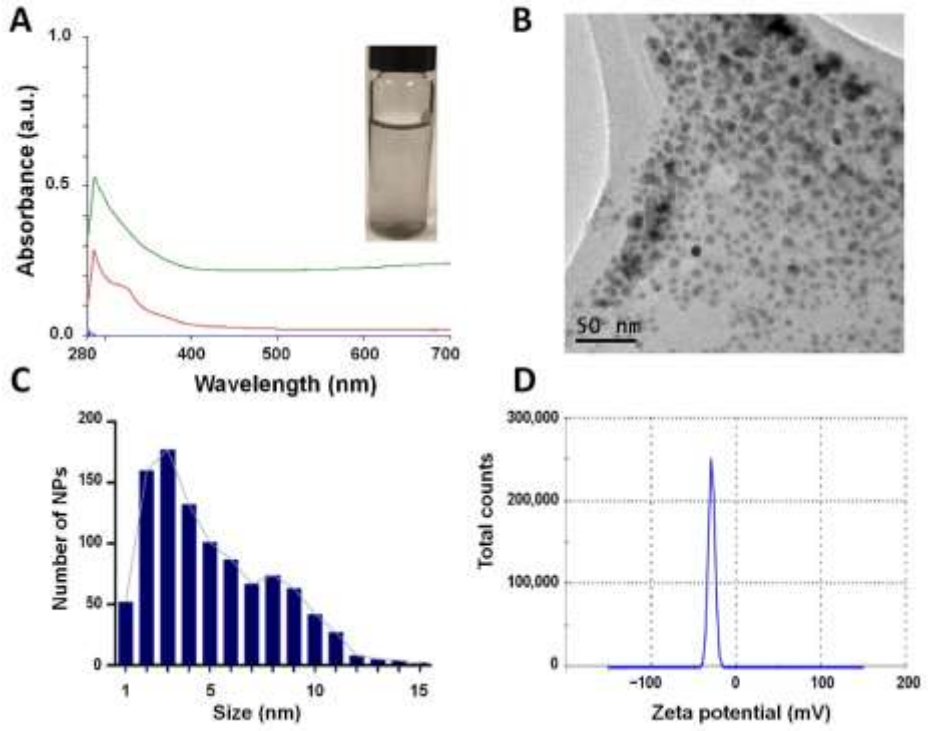

Figure 1. Characterization of CuONPs obtained with the supernatant of *G. sessile* (CuONPs-S). A) UV-Vis spectroscopy curves of CuONPs-S (green line) and supernatant (red line), inset shows nanoparticle suspension, B) TEM image of CuONPs-S showing quasi-spherical shape, C) size distribution histogram of CuONPs-S, D) Zeta potential.

By using the extract (CuONPs-E) a light blue color suspension was obtained, maximum absorbance peak was observed at 296.10 nm (Figure 2A), the blue color can be associated with Cu^{+2} species. Nanoparticles were polydisperse (PDI = 0.674) with quasi-spherical in morphology and seem to be embedded in a matrix of organic matter (Figure 2B) showing a size range between 1 to 20 nm (Figure 2C). The CuONPs-E nanoparticles exhibit –24.8 mV of zeta potential which can be associated with the capping biomolecules that surround the nanoparticles by polar functional groups with negative charge (Figure 2D). Z-potential values >30 are related usually with stable colloidal dispersion.

Preprints (www.preprints.org) | NOT PEER-REVIEWED | Posted: 11 July 2023 doi:10.20944/preprints202307.0734.v1

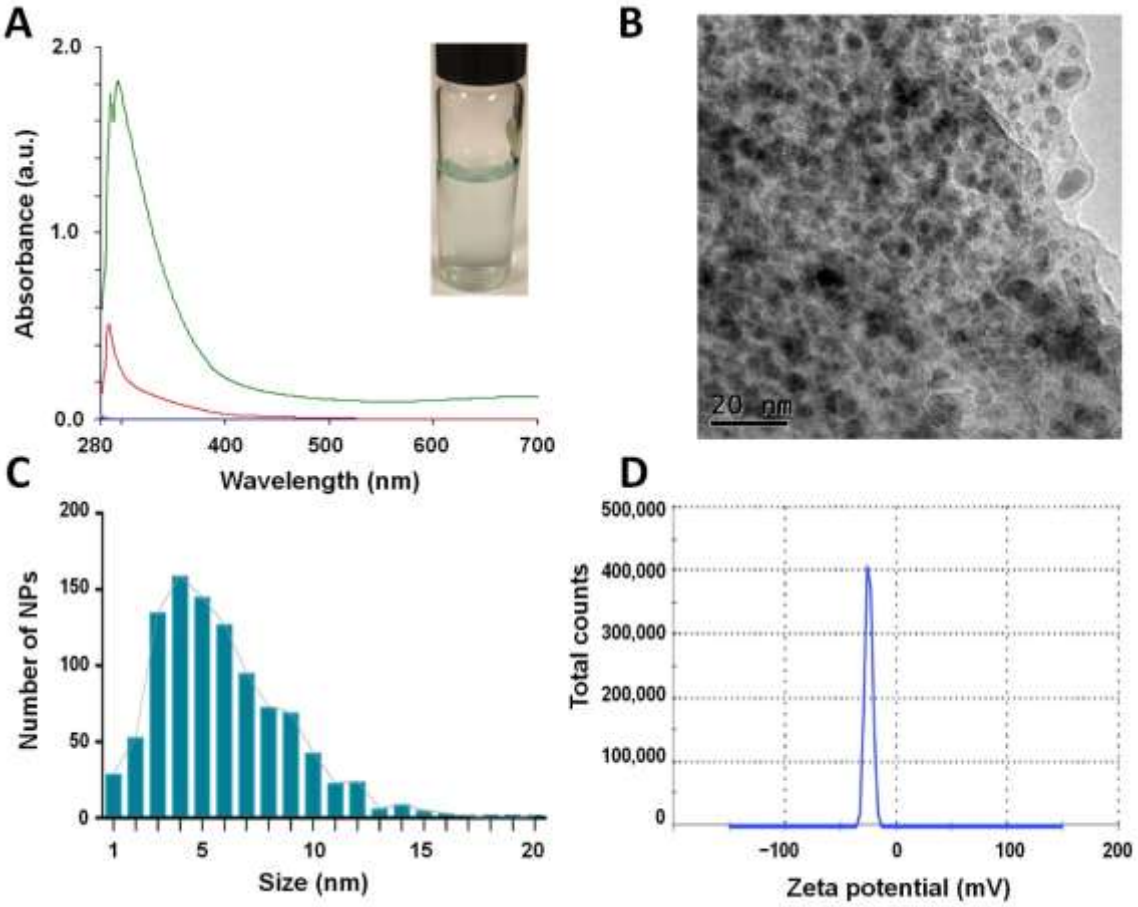

Figure 2. Characterization of CuONPs obtained with the extract of *G. sessile* (CuONPs-E). A) UV-Vis spectroscopy curves of CuONPs-E (green line) and supernatant (red line), inset shows nanoparticle

Preprints (www.preprints.org) | NOT PEER-REVIEWED | Posted: 11 July 2023 doi:10.20944/preprints202307.0734.v1

suspension; B) TEM image of CuONPs-E showing quasi-spherical shape and matrix of organic matter; C) size distribution histogram of CuONPs-E; D) Zeta potential of the CuONPs.

HRTEM images in Figure 3 correspond to CuONPs-S (Figure 3A) and CuONPs (Figure 3B), respectively. In is noticeable that copper oxide nanoparticles were embedded in biomass, suggesting that biomolecules, such as residual proteins and amino acids from the fungal act as a capping agent of the CuONPs. The lattice spacing in both micrographs (Figure 3A and 3B) was about 0.23 nm between the (111) plane, consistent with the monoclinic structure of the CuO (JCPDS Card no. 00-048-1548). The insets are the SAED patterns which revel the polycrystalline nature of the sample with (111) and $(20\bar{2})$ planes and diffuse rings that could be attributable to the presence capping biomolecules.

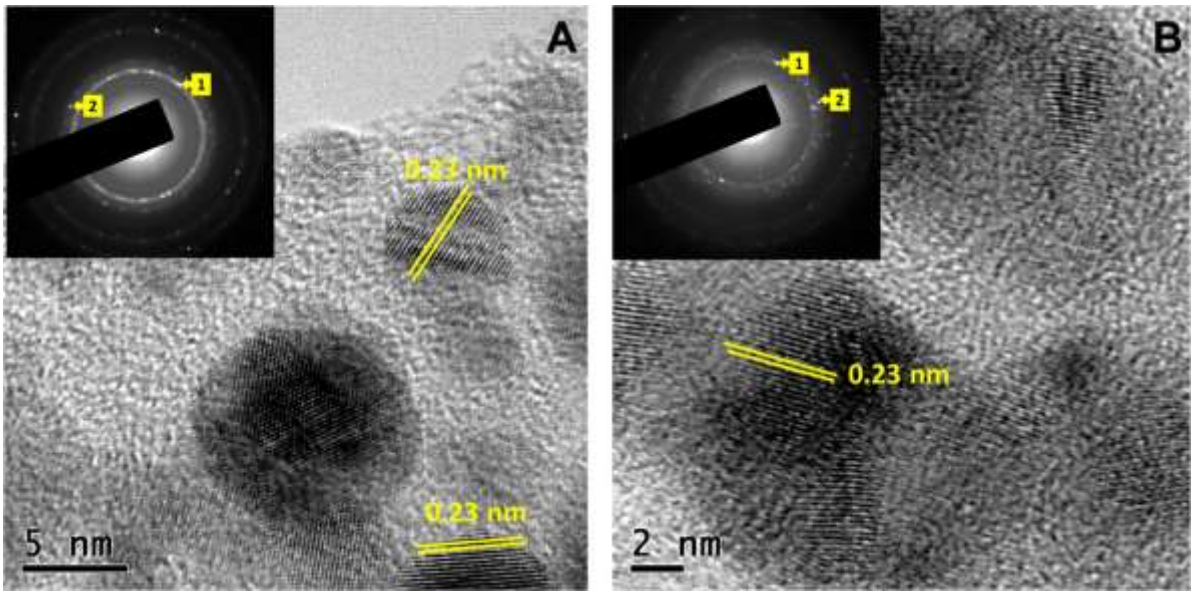

Figure 3. HRTEM images of CuONPs obtained with the supernatant (A: CuONPs-S) and extract (B:CuONPs-E) of *G. sessile*. The insets correspond to the SAED patterns of CuONPs-S and CuONPs respectively. .

3.2. X-ray diffraction (XRD) patterns of Synthesized CuONPs

The X-ray diffraction patterns of the biosynthesized CuONPs using the supernatant and extract of *G. sessile* are shown Figure 4. The noisy profiles of both patterns are usually associated with amorphous materials, in this case the biomolecules, such as residual proteins of *Ganoderma sessile* capping the CuO nanoparticles. The Bragg reflections show that the two samples have the same space group C2/c related with the monoclinic system of CuO. The peaks at $2\theta = 35.5°$, 38.7° and 48.7° were assigned to diffraction from the $(11\bar{1})$, (111) and $(20\bar{2})$ planes of the monoclinic structure of copper(II) oxide, which is in good agreement with the JCPDS Card No. 00-048-1548. Furthermore, additional reflections were detected, although exhibit low intensity signal in contrast with the CuO phase, can be associated with $Cu(NO_3)_2$ and the copper complex $[Cu(OH)_2NH_3H_2O]$ on the base of JCPDF Cards No. 00-019-0414 and 00-042-0637, respectively.

Preprints (www.preprints.org) | NOT PEER-REVIEWED | Posted: 11 July 2023 doi:10.20944/preprints202307.0734.v1

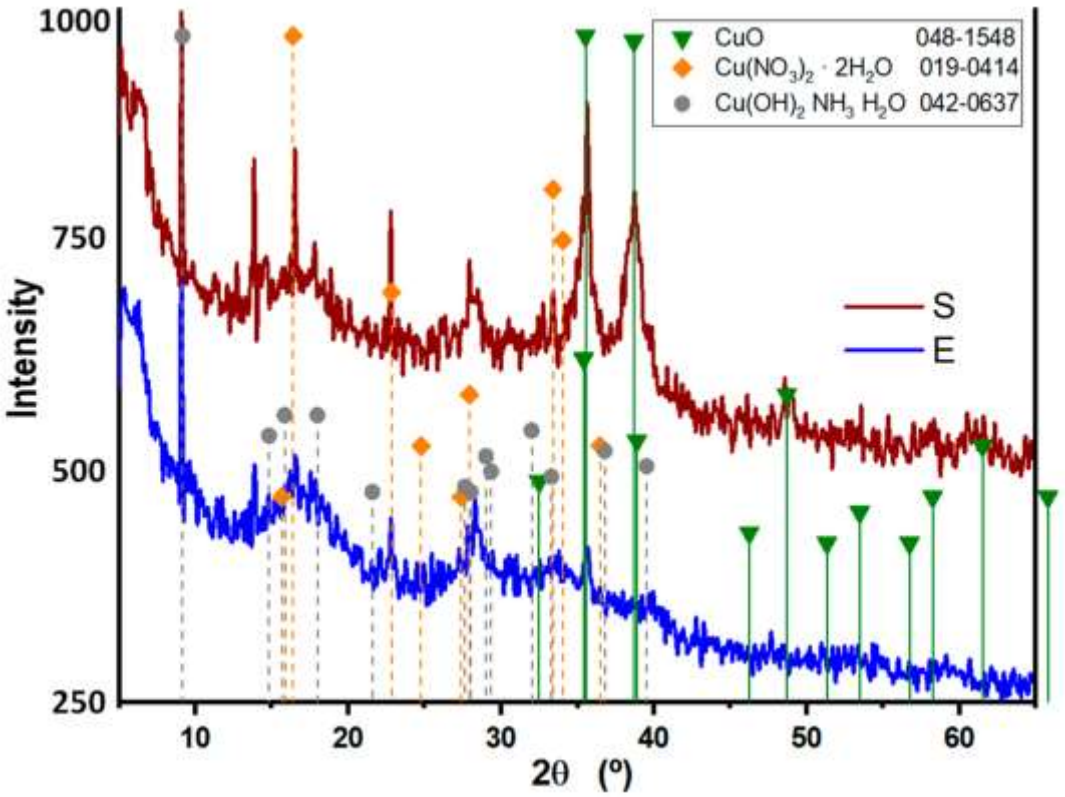

Figure 4. XRD spectrum of copper oxide nanoparticles obtained with the supernatant (S) and extract (E) of *G. sessile*.

3.3. FTIR Analysis of Synthesized CuONPs

Figure 5 shows the FTIR spectra of the CuONPs, the spectra exhibit two bands around 3387 and 3268 cm^{-1} has the characteristic appearance of compounds with N–H and OH groups [39]. The weak bands at 2972 and 2879 cm^{-1} are characteristic of stretching vibrations of methyl groups [40]. The peak at 1077 cm^{-1} spectrum was attributed to primary amines [40], which confirm the presence of residual amino acids and proteins from the fungus with are involved in the synthesis and stabilization of the copper oxide nanoparticles. Fungal supernatant and fungus extract is expected to contain amino acids, enzymes, and residual proteins, that might act as stabilization agent of the CuONPs, to support this both spectra in Figure 5 show a band at 471 cm^{-1} that corresponds to the stretching vibration of the bond Cu–N [40], indication that exist a strong interaction between the nanoparticles and the fungal biomolecules.

Preprints (www.preprints.org) | NOT PEER-REVIEWED | Posted: 11 July 2023 doi:10.20944/preprints202307.0734.v1

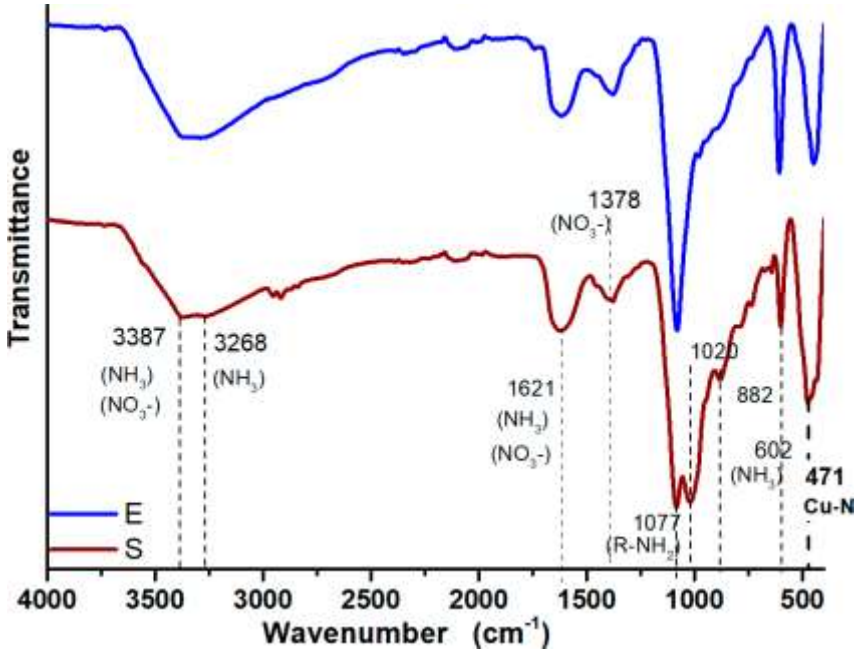

Figure 5. FTIR spectra of CuONPs obtained with the supernatant (S) and extract (E) of *G. sessile*.

3.4. Antibacterial capacity

Inhibition of bacteria exposed to CuONPs was observed for both Gram-negative and Gram-positive bacteria. Low concentrations of CuONPs were required for bacterial inhibition, IC50 was 10.2 and 8.8 µg/mL for *S. aureus*, 8.5 and 8.0 µg/mL for *E. coli*, and 4.1 and 3.4 µg/mL for *P. aeruginosa* (Table 1). As can be observed similar results were obtained when using both types of NPs, but *P. aeruginosa* was the most susceptible to both treatments (Figure 6). Although the MIC for bacterial strains were similar, slightly higher concentrations of CuONPs-E were required. The MIC obtained for *E. coli* and *S. aureus* was 15.9 µg/mL with CuONPs-S and 16.5 µg/mL using CuONPs-E. For *P. aeruginosa* a MIC of 13.7 µg/mL of CuONPs-S and 16.5 µg/mL of CuONPs-E was obtained (Figure 6).

Table 1. Physicochemical characteristics, antimicrobial effect, and toxicity analysis of CuONPs synthesized with the supernatant (S) and extract (E) of *G. sessile*.

NPs	Physicochemical characteristics				Antimicrobial effect						Toxicity		
	TEM		PDI	ZP (mV)	Bacteria (µg/mL)						Cell lines		
	Size (nm)	Shape			*E. coli*		*P. aeruginosa*		*S. aureus*		AML-12	RAW-264.7	MDCK
					MIC	IC50	MIC	IC50	MIC	IC50	IC50	IC50	IC50
CuONPs-S	4.5 ± 1.9	QS	0.619	-28.7	15.9	8.0	13.7	4.1	15.9	8.8	3.6	7.3	7.3
CuONPs-E	5.2 ± 2.1	QS	0.674	-24.8	16.5	8.5	16.5	3.4	16.5	10.2	14.7	29.5	29.5

NPs: nanoparticles, TEM: transmission electron microscopy, QS: quasi-spherical, PDI: polydispersity index, ZP: Zeta potential.

Preprints (www.preprints.org) | NOT PEER-REVIEWED | Posted: 11 July 2023 doi:10.20944/preprints202307.0734.v1

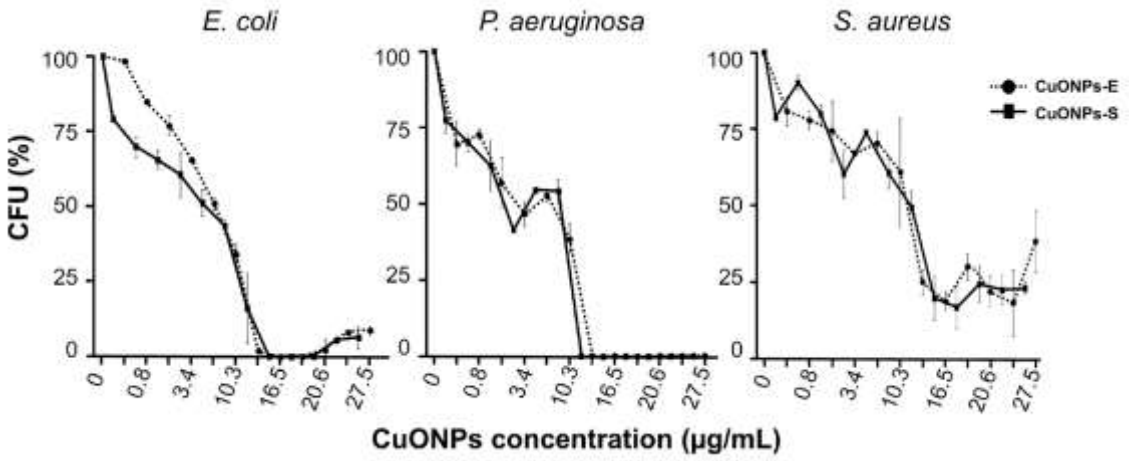

Figure 6. Antibacterial activity of CuONPs-S and CUONPs-E. Percentage of colony formation of bacteria recovered after treatment with CuONPs for 24 h.

3.3. ROS production in bacteria

ROS production was measured to determine if the exposure to CuONPs activates a stress response of oxidation in bacteria. We observed that at only at the highest concentration of NPs tested (close to the MIC obtained), the overproduction of ROS was higher (Figure 7). As shown in Figure 7, the ROS production at 0.62 µg/ml, 1.24 µg/ml of CuONPs, and the negative control is similar. Comparable stress was detected at 9.95, 4.97, 2.48, µg/mL (data not shown). In the case of *E. coli*, we can observe that at the highest concentration of NPs (19.9 µg/ml), the response is similar to the positive control. In general, *S. aureus* had the lower production of ROS at all CuONPs concentrations.

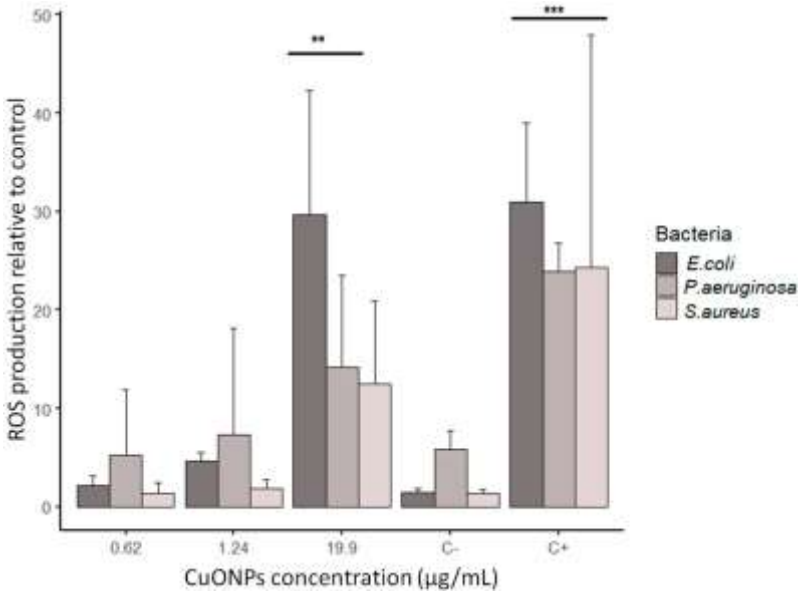

Figure 7. ROS production by bacteria exposed to CuONPs-S synthesized using *G. sessile*. C– = no treatment; C+ = positive control using 1 mM H_2O_2. Results are the mean +SD (n=3), ** $p < 0.01$; *** $p < 0.001$ (two-way ANOVA with a Dunnett's test).

3.4. Ultrastructural analysis of bacteria

To assess the interaction of CuONPs with bacterial cells, *E. coli* and *S. aureus* were exposed to the MIC and analyzed under TEM. At low magnifications it was difficult to detect NPs because mean size of NPs is about 5 nm. However, at higher magnifications it was detected that in all cases CuONPs

Preprints (www.preprints.org) | NOT PEER-REVIEWED | Posted: 11 July 2023 doi:10.20944/preprints202307.0734.v1

internalize into the cell. No specific accumulation was observed for *E. coli* (Figure 8A-B) or S. *aureus* (Figure 8C-D). However, NPs were detected throughout the cell and occasionally small accumulations were observed (Figure 8A-B). Control cultures were also analyzed to discard that any other material could be accumulated in cells treat with NPs and they were observed without any accumulation of foreign material (Figure 8E-H). Cells are observed with low contrast since no post-staining was used in order to easily detect small NPs.

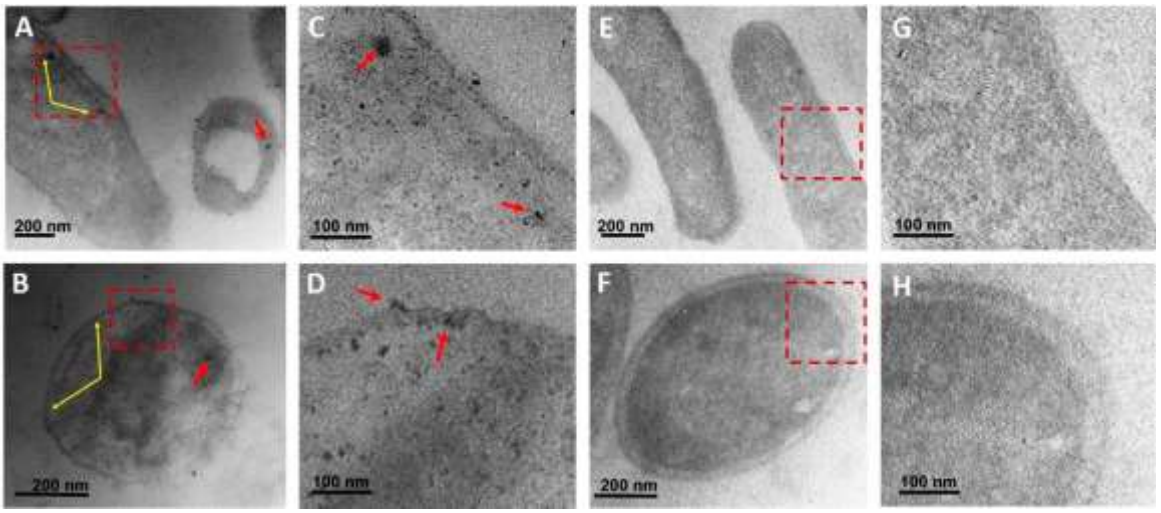

Figure 8. Ultrastructural analysis of bacteria exposed for 24 h to CuONPs biosynthesized using *G. sessile*. A-B) *E. coli* and *S. aureus* showing a high internal number of small NPs, respectively; C-D) Amplification of marked area in (A-B) showing in more detail the presence on NPs; E-F) Cells of *E. coli* and *S. aureus* from control cultures, without NPs treatment; G-H) Amplification of marked area in (E-F) showing no accumulation of any material. Red arrows indicate small accumulation of NPs, yellow arrows point out at slight accumulation of NPs within the cell wall and at the cell membrane.

3.5. Toxicity of CuONPs in Mammalian Cell Lines

To determine the cytotoxicity of the biosynthesized CuONPs, canine kidney (MDCK), murine macrophages (RAW 264.7) and murine hepatocytes (AML-12) were exposed to different volumes of CuONPs, cell viability was determined and reported at calculated final concentrations of CuONPs. As shown in Figure 9, cell viability was dose-dependent, and CuONPs-S were more cytotoxic than CUONPs-E. In addition, cell viability of hepatocytes treated with CuONPs-S were the most susceptible showing acceptable cell viability only at concentrations lower that 3.6 µg/mL, while using higher concentrations of CuONPs-E cell viability was higher at most concentrations used (Figure 9B). In the case of macrophages treated with CuONPs-S, also a decrease in cell viability was observed, proportional to the increase in the concentration of CuONPs-S, similar to that observed in hepatocytes. Macrophages treated with concentrations of 0.9 to 15.26 µg/mL of CuONPs-E did not induce any change in cell viability, however, at the concentration of 30.5 µg/mL of CuONPs-E causing a significant decrease of 14% in cell viability (Figure 9B). For kidney cells, CuONPs-S good cell viability was observed at concentrations up to 7.3 µg/mL (Figure 9A) while at concentrations of 14.7 and 29.5 µg/mL, the cell viability of kidney cells decreased drastically. However, excellent cell viability was observed in cells exposed to CuONPs-E, at concentrations between 0.9 µg/mL to 15.2 µg/mL of CuONPs, only at the highest concentration of 30.5 µg /mL the percentage of viability decreased at 55 % (Figure 9).

Preprints (www.preprints.org) | NOT PEER-REVIEWED | Posted: 11 July 2023 doi:10.20944/preprints202307.0734.v1

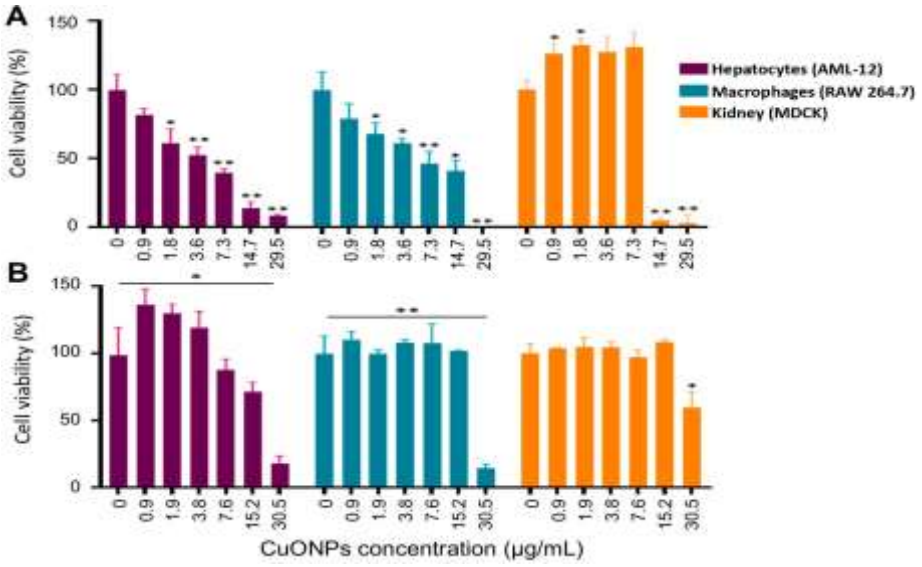

Figure 9. Cell viability assay in cell lines exposed to CuONPs-S (A) and CuONPs-E (B). Bars represent the mean + SD. * $p \geq 0.05$, ** $p \geq 0.01$.

To assess whether the cytotoxic effect observed in cell lines exposed to CuONPs-S and CuONPs-E was merely due to the NPs and not to the aqueous extract or supernatant of *G. sessile*, it was decided to compare the viability of hepatocytes, macrophages and kidney cells in the presence of two volumes of S and E, the lowest (0.7 µL) and the highest (22.2 µL) used for CuONPs, as well as the NPs synthesized from them. In the case of the cell lines treated with the supernatant, a slight decrease in cell viability was observed compared to the control, as shown in Figure 10. On the contrary, in hepatocytes and macrophages treated with the extract, an increase in cell viability was observed compared to the control, whereas in kidney cells, cell viability remained similar to the control.

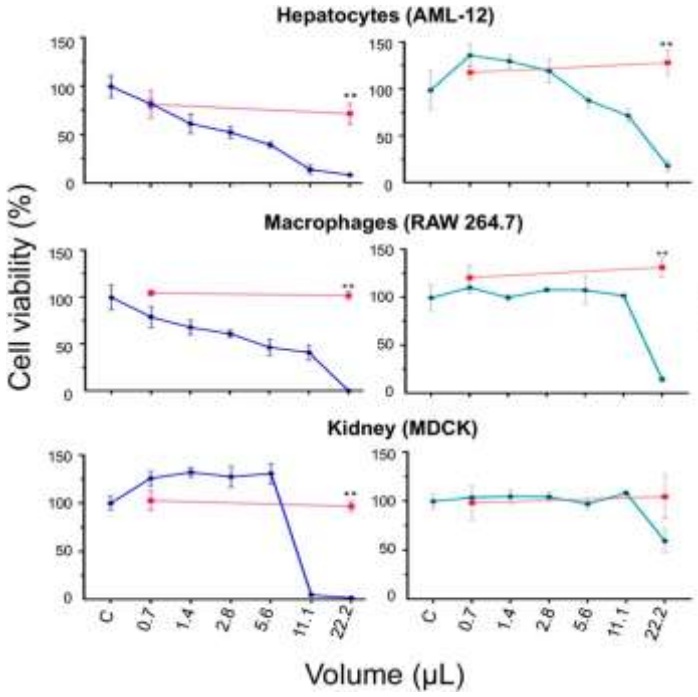

Figure 10. Cell viability assay in cell lines exposed to CuONPs-S (blue line) and CuONPs-E (cyan line). Red lines represent cell viability exposed to the fungal supernatant (left side) or extract (right side), respectively. ** $p \geq 0.01$.

Preprints (www.preprints.org) | NOT PEER-REVIEWED | Posted: 11 July 2023 doi:10.20944/preprints202307.0734.v1

4. Discussion

The biological synthesis of metallic NPs is considered an efficient and less toxic method [22,42]. Multiple studies report silver and gold NPs for biomedical applications, and recently copper oxide, zinc oxide, and iron oxide NPs are being considered [27–30]. The use of CuONPs has increased exponentially; they are being used in various applications such as industrial catalyst, gas sensors, electronic materials, biomedicine and environmental remediation [43]. Biosynthesized copper NPs have also been proposed for photocatalytic, antimicrobial, and optical sensor applications, among others [44–46]. Also, biosynthesized copper NPs have been reported for potential medical applications because of their anticancer, antimicrobial, antioxidant, and antidiabetic properties [9,31,32]. Furthermore, copper is an essential trace element for life processes like energy metabolism, reactive oxygen species detoxification, iron uptake, multiple enzymatic reactions and signaling in eukaryotic organisms [47,48]. Thus, copper is essential for life, but it is highly reactive and can cause cell damage, so cells have mechanisms for copper homeostasis and thus be able to maintain safe levels of this element [49]. However, it is well known that several factors provoke the toxicity of oxide NPs such as size, shape, surface modification and concentration [43].

Therefore, it is crucial to evaluate if biosynthesized copper NPs, using non-pathogenic fungi, can control pathogenic microorganisms and simultaneously have a low toxicity effect in mammalian cell lines. Previous studies have reported using fungi to biosynthesize copper nanoparticles (CuNPs). They were found to possess antimicrobial, antidiabetic, anticancer, and antioxidant properties [31,50,51].

In this work, we used *G. sessile*, which is considered as a non-photogenic fungus, in fact members of the *Ganoderma* family are considered as medicinal [52]. It is important to mention that the resulting biosynthesized nanomaterial is polydisperse in most cases; however, to obtain the desired size range and shape, the adjustment of the reaction conditions such as temperature, pH, time, and reaction mixture concentration is needed. The pH adjustment is crucial for the biosynthesis of CuNPs and CuONPs [31,51,53,54]. For example, Noor et al. [31], reported the pH adjustment for the synthesis of CuNPs using the extract of the fungus *Aspergillus niger* with $CuSO_4$. It was noted that when adjusting the pH to 5, 7 and 8, the synthesis of CuNPs was only achieved under a pH of 7. In the green synthesis of CuONPs using *Galphimia glauca* leaves and flowers extract, the authors observed that the most favorable pH for the synthesis of CuONPs was 12. While at low pH they reported that the activity of the carboxyl groups, present in the extract of *G. glauca* decreased in such a way that with a pH of 2 they obtained larger spherical CuONPs (50-60 nm) with a greater tendency to agglomeration [54]. The need to adjust the pH may be due to the decreased activity of reducing biomolecules due to the acidity of the precursor salt and/or the extract during the synthesis process. In this work, the pH of the 5 mM $CuSO_4.5H_2O$ solution was 3.72, while the pH of the mixture of the supernatant and extract of *G. sessile* with $CuSO_4.5H_2O$, was 3.18 and 3.37, respectively (ratio 1: 3). Therefore, for the synthesis of CuONPs using the aqueous extract and the supernatant of *G. sessile*, it was necessary to adjust the pH to 10.

The obtained CuONPs were analyzed using spectrophotometry in the UV-visible light range, and a maximum absorbance was found at 290.73 nm using the supernatant and 296.10 nm using the extract of *G. sessile*, similar to the maximum absorbance peak at 290 nm reported using the *Camellia japonica* leaf extract [45].

Regarding the sizes of the CuONPs, it was found that those obtained by TEM differ considerably from the hydrodynamic diameters obtained with DLS, which may be due to the adhesion of components (molecules, proteins) present in the extracts used from *G. sessile*. In addition, this material serves as a capping agent, which maintains the stability of NPs, evidenced by the zeta potential values (-28.7 and 24.8 mV for CuONPs-S and CuONPs-E, respectively).

Obtained nanoparticles were quasi spherical in shape, HRTEM and SAED analysis revealed their polycrystalline nature. The diffractograms revealed the presence of three copper compounds and both types of nanoparticles seem to have a considerable amorphous component, especially NPs made with the extract (E), this is expected from the biomass residues from the intracellular components. The copper(II) oxide signals, in NPs from the supernatant (S) are clearly visible, in NPs

Preprints (www.preprints.org) | NOT PEER-REVIEWED | Posted: 11 July 2023 doi:10.20944/preprints202307.0734.v1

from the extract (E) they are just resolved. The additional signals belong to copper nitrate and there are a couple of signals at low angles that seem to coincide with a complex of Cu with OH and NH_3, where could be due to the interaction of Cu+2 with OH and amino groups of the extract.

The profile of the FTIR spectra in the region between 3500 and 3250 cm^{-1} has the characteristic appearance of compounds with N–H, either ammonia or amines, this bond can be formed between Cu and protein residues. In fact, these results coincide with what was found in the DRX analysis.

The antibacterial activity of the CuONPs was determined through the bacterial growth inhibition assay, the MIC obtained was 16.5 μg/mL for all bacterial strains when using CuONPs-E. It is important to mention that both types of CuONPs were stable and maintained their antibacterial capacity for 2.5 years at ambient conditions. The concentrations needed for bacterial inhibition can be considered low, since higher concentrations of copper NPs for *E. coli* inhibition were reported by [55], the MIC obtained for different strains were in a range of 140 to 280 μg/mL for *E. coli*, 140 μg/mL for *S. aureus* and 20 μg/mL for *Bacillus subtilis*. In that study, the authors found that the Gram-positive *B. subtilis* strain MTCC 441 was more sensitive to the copper NPs, than silver NPs. Other studies report that CuNPs are not antibacterial at concentrations lower than 200 μg/mL with some Gram-negative bacteria, such as *E. coli* and *Salmonella typhimurium* [32].

Lipopeptide stabilized Cu_2O NPs of small size (30 ± 2 nm diameter) were reported to have antimicrobial activity against both Gram-positive and Gram-negative bacteria with a MIC of 62.5 μg/mL. Although, the IC50 reported was also higher than those concentrations reported in this study, they found 21.21 μg/L and 18.65 μg/mL for *P. aeruginosa* and *B. subtilis*, respectively [27].

Some of the proposed mechanisms of the antibacterial effect are through the interaction and disruption of the bacterial cell membrane, which allows the loss of cytoplasmic content [56,57]. In our study, although no evident specific accumulation of CuONPs was detected, in *E. coli* and *S. aureus* a slight accumulation in the cell wall and cytoplasmic membrane was found, this contrasts with the results of [27]. They reported that the ultrastructure of *B. subtilis* and *P. aeruginosa* remarkably changed after exposure to cuprous oxide NPs. They found a high accumulation of NPs attached to the surface of *B. subtilis*, displaying low density regions due to permeability of the cell wall and leakage of cytoplasmic content. However, bacteria were exposed to higher concentrations and different type of NPs, lipopeptide stabilized Cu_2ONPs with a higher average size (30 ± 2 nm) were used [27].

CuNPs have been reported to cause multiple toxic effects in *E. coli* cells, such as the generation of ROS, lipid peroxidation, protein oxidation and DNA degradation [58]. In addition, the antibacterial activity of CuNPs evaluated in *E. coli* and *Proteus vulgaris* revealed a dose-dependent bactericidal action. Exposure to NPs provoked ROS generation, loss of membrane permeability and finally leakage of cytoplasmic components. Those effects were reported as the cause of CuNP-induced bacterial cell death [57].

Concerning to the oxidative stress that nanometals could cause to bacteria, it is well documented that elevated ROS production occurs when bacteria is exposed to high concentrations of AgNPs and Cu/CuONPs [57–61]. The same was true in our study, although we used relatively low concentrations of CuONPs, we detected elevated ROS production in all bacteria only at the highest concentration of CuONPs tested.

It is possible that the ROS overproduction at relatively low concentrations of CuONPs is associated with the material used to biosynthesize our NPs; this could be related to the ability of organic molecules (present in the supernatant/extract) to interact with cell membranes. We need to investigate the hydrophilicity/hydrophobicity interactions between molecules contained in the fungal extracts herein used, which could be crucial to overpassing the natural barriers in cells. Indeed, ions produced by metals can interact with some electrons in the molecules of cells membranes, but it is probably that a synergic effect is produced by using the organic molecules in the extract and supernatant of *G. sessile*, that provide the NPs a surface corona that can interact with biological systems [62–64].

Nanometal oxides such as ZnO and CuO NPs synthesized by a sol–gel combustion route, were reported as excellent antibacterial agents against both Gram-positive and Gram-negative bacteria.

Preprints (www.preprints.org) | NOT PEER-REVIEWED | Posted: 11 July 2023 doi:10.20944/preprints202307.0734.v1

However, the authors stated the importance of identifying the key physicochemical properties of nanometal oxides that govern antibacterial capacity and also the cytotoxicity to mammalian cells [65].

In this respect, cellular toxicity produced by metal oxide NPs is well documented [12,66,67]. However, the specific mechanisms of this toxicity are not yet fully described. There are different theories of the toxic effect on animal cells, one of them is based on the production of reactive oxygen species (ROS) as one of the determining factors of cell death [54]. In this way, in the biomedical area, metallic NPs can act as a therapeutic agent and consider this toxic property as an undesired effect. Nevertheless, this toxic effect could be useful to limit and control highly lethal cancers. However, in some of the biomedical applications of CuONPs, and other metallic NPs, it is necessary to focus on minimizing toxicity. In such cases, CuONPs can be embedded in materials for medical use, providing the antibacterial effect only on contact with the surface, but without generating toxicity in those who handle it [68,69]. To reduce toxicity, in this study we used fungal supernatant and extract of a non-pathogenic fungus, which proved to have no-toxic response in three mammalian cell lines (Figure 9). Nevertheless, CuONPs-E were less toxic for mammalian cells lines with IC50 of 29.5 μg/mL for macrophages and kidney cells, and for hepatocytes the IC50 was 14.7 μg/mL, close to the MIC found for bacteria (16.5 μg/mL). Then, these concentrations of Cu could be considered safe for humans since the World Health Organization (WHO) reported a value of 2.0 mg/L as a regulation or guideline for copper in drinking water [70]. Also, only at high concentrations of Cu, animal studies have shown liver injury and inflammatory responses to Cu administered above 4 mg/kg/day [71].

It is important to identify the degree of toxicity that CuONPs can produce, regardless of the synthesis method to produce them. Determining the toxic concentrations of CuONPs will allow knowing the safe concentrations for future applications in the biomedical area. In this work, the CuONPs synthesized with the extract proved to be less toxic than the CuONPs synthesized with the supernatant of *G. sessile*, allowing the appropriate selection for future applications.

5. Conclusions

CuONPs were successfully obtained using the extracellular metabolites (supernatant) and the intracellular components (extract) of the fungus *G. sessile*. The antibacterial property against pathogenic bacteria makes them a possible eco-friendly alternative for managing of infectious diseases since CuONPs were stable and maintained their antibacterial capacity for 2.5 years at ambient conditions. Cell viability results indicate that low concentrations (<15 μg/mL) of CuONPs are not toxic to kidney and macrophage cell lines and have an IC50 of 14.7 μg/mL for hepatocytes. This demonstrates the biocompatibility of the biosynthesized CuONPs and makes them excellent candidates for the treatment of superficial infectious diseases. However, it would be necessary to demonstrate that they have a low absorption into the systemic circulation, and consequently a low concentration during renal excretion.

Author Contributions: E.C.-L. contributed to conceptualization and study design. K.M.F.-R and D.R.-M. contributed to the implementation of experimental protocols. K.J.-M. contributed to the implementation and supervision of experimental protocols. A.R.V.-N contributed to the supervision of experimental protocols. All authors have read and agreed to the published version of the manuscript.

Funding: This research received no external funding.

Institutional Review Board Statement: Not applicable.

Informed Consent Statement: Not applicable.

Acknowledgments: We thank CONACyT for a scholarship for K.M.F.-R. and D.R.-M. We also acknowledge the LNMA of CICESE and Dr. Gabriela Guzmán for technical help. This research was partially supported by CONACYT Grant A1-S-34533.

Conflicts of Interest: The authors declare no conflict of interest.

Preprints (www.preprints.org) | NOT PEER-REVIEWED | Posted: 11 July 2023 doi:10.20944/preprints202307.0734.v1

References

1. Blecher, K., Nasir, A., Friedman, A. 2011. The growing role of nanotechnology in combating infectious disease. Virulence, 2(5), 395–401.
2. Farokhzad, O. C., Langer, R. 2009. Impact of nanotechnology on drug delivery. ACS Nano, 3(1), 16–20. doi:10.1021/nn900002m
3. Kaweeteerawat, C., Na Ubol, P., Sangmuang, S., Aueviriyavit, S., Maniratanachote, R. 2017. Mechanisms of antibiotic resistance in bacteria mediated by silver nanoparticles. Journal of Toxicology and Environmental Health - Part A: Current Issues, 80(23–24), 1276–1289. doi:10.1080/15287394.2017.1376727
4. Pelgrift, R. Y., Friedman, A. J. 2013. Nanotechnology as a therapeutic tool to combat microbial resistance. Advanced Drug Delivery Reviews, 65(13–14), 1803–1815. doi:10.1016/j.addr.2013.07.011
5. Zhang, L., Gu, F., Chan, J., Wang, A., Langer, R., Farokhzad, O. 2007. Therapeutic, Nanoparticles in Medicine: Applications and Developments. Education Policy Analysis Archives, 8(5), 761–769. doi:10.1038/sj.clp
6. Alizadeh, S., Seyedalipour, B., Shafieyan, S., Kheime, A., Mohammadi, P., Aghdami, N. 2019. Copper nanoparticles promote rapid wound healing in acute full thickness defect via acceleration of skin cell migration, proliferation, and neovascularization. Biochemical and Biophysical Research Communications, 517(4), 684–690. doi:10.1016/j.bbrc.2019.07.110
7. Lu, Y., Lihua, L., Zhu, Y., Wang, X., Li, M., Zefeng, L., Xiaoming, H., Zhang, Y., Qingshiu, Y., Chuanbin, M. 2018. Multifunctional copper-containing carboxymethyl chitosan/alginate scaffolds for eradicating clinical bacterial infection and promoting bone formation. ACS Applied Materials and Interfaces, 10(1), 127–138. doi:10.1021/acsami.7b13750.
8. Norambuena, G. A., Patel, R., Karau, M., Wyles, C. C., Jannetto, P. J., Bennet, K. E., Hanssen, A. D., Sierra, R. J. 2017. Antibacterial and Biocompatible Titanium-Copper Oxide Coating May Be a Potential Strategy to Reduce Periprosthetic Infection: An In Vitro Study. Clinical Orthopaedics and Related Research, 475(3), 722–732. doi:10.1007/s11999-016-4713-7
9. Rajeshkumar, S., Menon, S., Venkat Kumar, S., Tambuwala, M. M., Bakshi, H. A., Mehta, M., Satija, S., Gupta, G., Chellappan, D. K., Thangavelu, L., Dua, K. 2019. Antibacterial and antioxidant potential of biosynthesized copper nanoparticles mediated through Cissus arnotiana plant extract. Journal of Photochemistry and Photobiology B: Biology, 197(May). doi:10.1016/j.jphotobiol.2019.111531
10. Lee J, Choi KH, Min J, Kim HJ, Jee JP, Park BJ. 2017. Functionalized ZnO nanoparticles with gallic acid for antioxidant and antibacterial activity against methicillin resistant S. Aureus. Nanomaterials 7(11):365. doi: 10.3390/nano7110365.
11. Lakshmi KR, Sri Venkata NP, Girija SG, Veerabhadra SP, Venkata RMK. 2019. A review on anti-bacterials to combat resistance: from ancient era of plants and metals to present and future perspectives of green nano technological combinations. Asian J Pharm Sci.7:1–18. doi: 10.1016/j.ajps.2019.03.002.
12. Henson, T. E., Navratilova, J., Tennant, A. H., Bradham, K. D., Rogers, K. R., Hughes, M. F. 2019. In vitro intestinal toxicity of copper oxide nanoparticles in rat and human cell models. Nanotoxicology, 13(6), 795–811. doi:10.1080/17435390.2019.1578428
13. Midander, K., Cronholm, P., Karlsson, H. L., Elihn, K., Möller, L., Leygraf, C., Wallinder, I. O. 2009. Surface characteristics, copper release, and toxicity of nano- and micrometer-sized copper and copper(ll) oxide particles: A cross-disciplinary study. Small, 5(3), 389–399. doi:10.1002/smll.200801220
14. Ramesh, M., Anbuvannan, M., & Viruthagiri, G. J. S. A. P. A. M. (2015). Green synthesis of ZnO nanoparticles using Solanum nigrum leaf extract and their antibacterial activity. Spectrochimica Acta Part A: Molecular and Biomolecular Spectroscopy, 136, 864-870.
15. Vijayakumar, V., Samal, S. K., Mohanty, S., Nayak, S. K. 2019. Recent advancements in biopolymer and metal nanoparticle-based materials in diabetic wound healing management. International Journal of Biological Macromolecules, 122, 137–148. doi:10.1016/j.ijbiomac.2018.10.120
16. Oskam, G. (2006). Metal oxide nanoparticles: synthesis, characterization and application. Journal of sol-gel science and technology, 37, 161-164.
17. Gour, A., Jain, N. K. 2019. Advances in green synthesis of nanoparticles. Artificial Cells, Nanomedicine and Biotechnology, 47(1), 844–851. doi:10.1080/21691401.2019.1577878
18. Andra, S., Balu, S. K., Jeevanandham, J., Muthalagu, M., Vidyavathy, M., Chan, Y. S., & Danquah, M. K. (2019). Phytosynthesized metal oxide nanoparticles for pharmaceutical applications. Naunyn-Schmiedeberg's archives of pharmacology, 392, 755-771.
19. Hussain, I., Singh, N. B., Singh, A., Singh, H., Singh, S. C. 2016. Green synthesis of nanoparticles and its potential application. Biotechnology Letters, 38(4), 545–560. doi:10.1007/s10529-015-2026-7
20. Kharissova, O. V., Dias, H. V. R., Kharisov, B. I., Pérez, B. O., Pérez, V. M. J. 2013. The greener synthesis of nanoparticles. Trends in Biotechnology, 31(4), 240–248. doi:10.1016/j.tibtech.2013.01.003

Preprints (www.preprints.org) | NOT PEER-REVIEWED | Posted: 11 July 2023 doi:10.20944/preprints202307.0734.v1

21. Shafey, A. M. E. (2020). Green synthesis of metal and metal oxide nanoparticles from plant leaf extracts and their applications: A review. Green Processing and Synthesis, 9(1), 304-339.
22. Castro-Longoria, E. 2016. Fungal Biosynthesis of Nanoparticles, a Cleaner Alternative. In Fungal Applications in Sustainable Environmental Biotechnology; Springer: Berlin/Heidelberg, Germany, pp. 323–351.
23. Abdel-Wareth, M. T. A. 2017. Fungal applications in sustainable environmental biotechnology. En International Journal of Environmental Studies. doi:10.1080/00207233.2017.1363570
24. Dhillon, G. S., Brar, S. K., Kaur, S., Verma, M. 2012. Green approach for nanoparticle biosynthesis by fungi: Current trends and applications. Critical Reviews in Biotechnology, 32(1), 49–73. doi:10.3109/07388551.2010.550568
25. Vetchinkina, E., Loshchinina, E., Kupryashina, M., Burov, A., Pylaev, T., Nikitina, V. 2018. Green synthesis of nanoparticles with extracellular and intracellular extracts of basidiomycetes. PeerJ, 2018(7). doi:10.7717/peerj.5237
26. Murillo-Rábago, E. I., Vilchis-Nestor, A. R., Juarez-Moreno, K., Garcia-Marin, L. E., Quester, K., & Castro-Longoria, E. (2022). Optimized synthesis of small and stable silver nanoparticles using intracellular and extracellular components of fungi: An alternative for bacterial inhibition. Antibiotics, 11(6), 800.
27. Bezza, F. A., Tichapondwa, S. M., & Chirwa, E. M. (2020). Fabrication of monodispersed copper oxide nanoparticles with potential application as antimicrobial agents. Scientific Reports, 10(1), 16680.
28. Ashraf, N., Ahmad, F., Da-Wei, L., Zhou, R. Bin, Feng-Li, H., Yin, D. C. 2019. Iron/iron oxide nanoparticles: advances in microbial fabrication, mechanism study, biomedical, and environmental applications. Critical Reviews in Microbiology, 45(3), 278–300. doi:10.1080/1040841X.2019.1593101
29. Dadfar, S. M., Roemhild, K., Drude, N. I., von Stillfried, S., Knüchel, R., Kiessling, F., Lammers, T. 2019. Iron oxide nanoparticles: Diagnostic, therapeutic and theranostic applications. Advanced Drug Delivery Reviews, 138, 302–325. doi:10.1016/j.addr.2019.01.005
30. Jamdagni, P., Khatri, P., Rana, J. S. 2018. Green synthesis of zinc oxide nanoparticles using flower extract of Nyctanthes arbor-tristis and their antifungal activity. Journal of King Saud University - Science, 30(2), 168–175. doi:10.1016/j.jksus.2016.10.002
31. Noor, S., Shah, Z., Javed, A., Ali, A., Hussain, S. B., Zafar, S., Ali, H., Muhammad, S. A. 2020. A fungal based synthesis method for copper nanoparticles with the determination of anticancer, antidiabetic and antibacterial activities. Journal of Microbiological Methods, 174(March), 105966. doi:10.1016/j.mimet.2020.105966
32. Erci, F., Cakir-Koc, R., Yontem, M., Torlak, E. 2020. Synthesis of biologically active copper oxide nanoparticles as promising novel antibacterial-antibiofilm agents. Preparative Biochemistry and Biotechnology, 6068. doi:10.1080/10826068.2019.1711393
33. Nikolova, M. P., & Chavali, M. S. (2020). Metal oxide nanoparticles as biomedical materials. Biomimetics, 5(2), 27.
34. Sharma, Purva, Tulsawani, R. 2020. Ganoderma lucidum aqueous extract prevents hypobaric hypoxia induced memory deficit by modulating neurotransmission, neuroplasticity and maintaining redox homeostasis. Scientific Reports, 10(1), 1–16. doi:10.1038/s41598-020-65812-5
35. Vetchinkina, E., Shirokov, A., Bucharskaya, A., Navolokin, N., Prilepskii, A., Burov, A., Maslyakova, G., Nikitina, V. 2016. Antitumor activity of extracts from medicinal basidiomycetes mushrooms. International Journal of Medicinal Mushrooms, 18(11), 955–964. doi:10.1615/IntJMedMushrooms.v18.i11.10
36. CLSI. 2012. Methods for Dilution Antimicrobial Susceptibility Tests for Bacteria That Grow Aerobically; Approved Standard—Ninth Edition (CLSI docum, Vol. 32). Clinical and Laboratory Standards Institute: Wayne, PA.
37. Wiegand, I., Hilpert, K., & Hancock, R. E. (2008). Agar and broth dilution methods to determine the minimal inhibitory concentration (MIC) of antimicrobial substances. Nature protocols, 3(2), 163-175.
38. Vazquez-Muñoz, R., Avalos-Borja, M., & Castro-Longoria, E. (2014). Ultrastructural analysis of Candida albicans when exposed to silver nanoparticles. PloS one, 9(10), e108876.
39. Nakamoto, K. (2009). Infrared and Raman spectra of inorganic and coordination compounds, part B: applications in coordination, organometallic, and bioinorganic chemistry. John Wiley & Sons, 6th edition.
40. Skoog, D. A., Holler, F. J., & Crouch, S. R. (2017). Principles of instrumental analysis. Cengage learning.
41. Hathaway, B. J., & Tomlinson, A. A. G. (1970). Copper (II) ammonia complexes. Coordination Chemistry Reviews, 5(1), 1-43.
42. Quester, K., Avalos-Borja, M., & Castro-Longoria, E. (2013). Biosynthesis and microscopic study of metallic nanoparticles. Micron, 54, 1-27.
43. Naz, S., Gul, A., & Zia, M. (2020). Toxicity of copper oxide nanoparticles: a review study. IET nanobiotechnology, 14(1), 1-13.

Preprints (www.preprints.org) | NOT PEER-REVIEWED | Posted: 11 July 2023 doi:10.20944/preprints202307.0734.v1

44. Mali, S. C., Dhaka, A., Githala, C. K., Trivedi, R. 2020. Green synthesis of copper nanoparticles using Celastrus paniculatus Willd. leaf extract and their photocatalytic and antifungal properties. Biotechnology Reports, 27, e00518. doi:10.1016/j.btre.2020.e00518
45. Maruthupandy, M., Zuo, Y., Chen, J. S., Song, J. M., Niu, H. L., Mao, C. J., Zhang, S. Y., Shen, Y. H. 2017. Synthesis of metal oxide nanoparticles (CuO and ZnO NPs) via biological template and their optical sensor applications. Applied Surface Science, 397, 167–174. doi:10.1016/j.apsusc.2016.11.118
46. Sivaraj, R., Rahman, P. K. S. M., Rajiv, P., Salam, H. A., Venckatesh, R. 2014. Biogenic copper oxide nanoparticles synthesis using Tabernaemontana divaricate leaf extract and its antibacterial activity against urinary tract pathogen. Spectrochimica Acta - Part A: Molecular and Biomolecular Spectroscopy, 133, 178–181. doi:10.1016/j.saa.2014.05.048
47. Scheiber, I. F., Mercer, J. F. B., Dringen, R. 2014. Metabolism and functions of copper in brain. Progress in Neurobiology, 116, 33–57. doi:10.1016/j.pneurobio.2014.01.002
48. Ruiz, L. M., Libedinsky, A., & Elorza, A. A. (2021). Role of copper on mitochondrial function and metabolism. Frontiers in molecular biosciences, 8, 711227.
49. Barber, R. G., Grenier, Z. A., & Burkhead, J. L. (2021). Copper toxicity is not just oxidative damage: Zinc systems and insight from Wilson disease. Biomedicines, 9(3), 316.
50. El-Batal, A. I., Al-Hazmi, N. E., Mosallam, F. M., El-Sayyad, G. S. 2018. Biogenic synthesis of copper nanoparticles by natural polysaccharides and Pleurotus ostreatus fermented fenugreek using gamma rays with antioxidant and antimicrobial potential towards some wound pathogens. Microbial Pathogenesis, 118, 159–169. doi:10.1016/j.micpath.2018.03.013
51. Honary, S., Barabadi, H., Gharaei-Fathabad, E., Naghibi, F. 2012. Green synthesis of copper oxide nanoparticles using Penicillium aurantiogriseum, Penicillium citrinum and Penicillium waksmanii. Digest Journal of Nanomaterials and Biostructures, 7(3), 999–1005.
52. Bishop, K.S.; Kao, C.H.; Xu, Y.; Glucina, M.P.; Paterson, R.R.M.; Ferguson, L.R. From 2000 years of Ganoderma lucidum to recent developments in nutraceuticals. Phytochemistry 2015, 114, 56–65.
53. Consolo, V. F., Torres-Nicolini, A., Alvarez, V. A. 2020. Mycosinthetized Ag, CuO and ZnO nanoparticles from a promising Trichoderma harzianum strain and their antifungal potential against important phytopathogens. Scientific Reports, 10(1), 1–9. doi:10.1038/s41598-020-77294-6
54. Oza, G., Calzadilla-Avila, A. I., Reyes-Calderón, A., Anna, K. K., Ramírez-Bon, R., Tapia-Ramirez, J., Sharma, A. 2020. pH-dependent biosynthesis of copper oxide nanoparticles using Galphimia glauca for their cytocompatibility evaluation. Applied Nanoscience (Switzerland), 10(2), 541–550. doi:10.1007/s13204-019-01159-2
55. Ruparelia, J. P., Chatterjee, A. K., Duttagupta, S. P., & Mukherji, S. (2008). Strain specificity in antimicrobial activity of silver and copper nanoparticles. Acta biomaterialia, 4(3), 707-716.
56. Ameh, T., Sayes, C. M. 2019. The potential exposure and hazards of copper nanoparticles: A review. Environmental Toxicology and Pharmacology, 71(June), 103220. doi:10.1016/j.etap.2019.103220
57. Sharma, P., Goyal, D., & Chudasama, B. (2022). Antibacterial activity of colloidal copper nanoparticles against Gram-negative (Escherichia coli and Proteus vulgaris) bacteria. Letters in Applied Microbiology, 74(5), 695-706.
58. Chatterjee, A. K., Chakraborty, R., & Basu, T. (2014). Mechanism of antibacterial activity of copper nanoparticles. Nanotechnology, 25(13), 135101.
59. Choi, O., & Hu, Z. (2008). Size dependent and reactive oxygen species related nanosilver toxicity to nitrifying bacteria. *Environmental Science & Technology, 42(12), 4583–4588. https://doi.org/10.1021/es703238h*
60. Quinteros, M. A., Cano Aristizábal, V., Dalmasso, P. R., Paraje, M. G., & Páez, P. L. (2016). Oxidative stress generation of silver nanoparticles in three bacterial genera and its relationship with the antimicrobial activity. *Toxicology in Vitro, 36, 216–223. https://doi.org/10.1016/j.tiv.2016.08.007*
61. Ameh, T., Gibb, M., Stevens, D., Pradhan, S. H., Braswell, E., & Sayes, C. M. (2022). Silver and copper nanoparticles induce oxidative stress in bacteria and mammalian cells. Nanomaterials, 12(14), 2402.
62. Peetla, C., Stine, A., & Labhasetwar, V. (2009). Biophysical interactions with model lipid membranes: Applications in drug discovery and drug delivery. *Molecular Pharmaceutics, 6(5), 1264–1276. https://doi.org/10.1021/mp9000662*
63. Le-Deygen, I. M., Safronova, A. S., Mamaeva, P. V., Kolmogorov, I. M., Skuredina, A. A., & Kudryashova, E. V. (2022). Drug–membrane interaction as revealed by spectroscopic methods: The role of drug structure in the example of rifampicin, levofloxacin and rapamycin. *Biophysica, 2(4), 353–365. https://doi.org/10.3390/biophysica2040032*
64. Singh, P., Kim, Y.-J., Zhang, D., & Yang, D.-C. (2016). Biological synthesis of nanoparticles from plants and microorganisms. *Trends in Biotechnology, 34(7), 588–599. https://doi.org/10.1016/j.tibtech.2016.02.006*

Preprints (www.preprints.org) | NOT PEER-REVIEWED | Posted: 11 July 2023 doi:10.20944/preprints202307.0734.v1

65. Azam, A., Ahmed, A. S., Oves, M., Khan, M. S., Habib, S. S., & Memic, A. (2012). Antimicrobial activity of metal oxide nanoparticles against Gram-positive and Gram-negative bacteria: a comparative study. International journal of nanomedicine, 6003-6009.
66. Bondarenko, O., Juganson, K., Ivask, A., Kasemets, K., Mortimer, M., & Kahru, A. (2013). Toxicity of Ag, CuO and ZnO nanoparticles to selected environmentally relevant test organisms and mammalian cells in vitro: a critical review. Archives of toxicology, 87, 1181-1200.
67. Yu, Z., Li, Q., Wang, J., Yu, Y., Wang, Y., Zhou, Q., Li, P. 2020. Reactive Oxygen Species-Related Nanoparticle Toxicity in the Biomedical Field. Nanoscale Research Letters, 15(1). doi:10.1186/s11671-020-03344-7
68. Humphreys, H. 2014. Self-disinfecting and microbiocide-impregnated surfaces and fabrics: What potential in interrupting the spread of healthcare-associated infection? Clinical Infectious Diseases, 58(6), 848–853. doi:10.1093/cid/cit765
69. Mitra, D., Kang, E. T., Neoh, K. G. 2020. Antimicrobial Copper-Based Materials and Coatings: Potential Multifaceted Biomedical Applications. ACS Applied Materials and Interfaces, 12(19), 21159–21182. doi:10.1021/acsami.9b17815
70. World Health Organization. (2021). A global overview of national regulations and standards for drinking-water quality.
71. Liu, H.; Guo, H.; Deng, H.; Cui, H.; Fang, J.; Zuo, Z.; Deng, J.; Li, Y.;Wang, X.; Zhao, L. Copper Induces Hepatic Inflammatory Responses by Activation of MAPKs and NF-KB Signalling Pathways in the Mouse. Ecotoxicol. Environ. Saf. 2020, 201, 110806.

Disclaimer/Publisher's Note: The statements, opinions and data contained in all publications are solely those of the individual author(s) and contributor(s) and not of MDPI and/or the editor(s). MDPI and/or the editor(s) disclaim responsibility for any injury to people or property resulting from any ideas, methods, instructions or products referred to in the content.